Microelectronic Engineering 88 (2011) 240–246

Contents lists available at ScienceDirect

Microelectronic Engineering

journal homepage: www.elsevier.com/locate/mee

Imprint lithography enabling ultra-low loss coaxial interconnects

Venmathy Rajarathinam, Nathan Fritz, Sue Ann Bidstrup Allen, Paul A. Kohl *

School of Chemical & Biomolecular Engineering, Georgia Institute of Technology, 311 Ferst Drive, Atlanta, GA 30332-0100, United States

ARTICLE INFO

Article history:
Received 1 July 2010
Received in revised form 21 October 2010
Accepted 31 October 2010
Available online 9 November 2010

Keywords:
Interconnects
Air dielectrics
Sacrificial polymers
Imprint lithography

ABSTRACT

Processing techniques have been demonstrated to fabricate a novel structure with smooth transitions, metallic shielding, and encapsulated air dielectric layers using sacrificial polymers and the three-dimensional patterning capabilities of imprint lithography. This innovative structure incorporates encapsulated air dielectrics with copper shielding. A semicircular stamp was fabricated to create the circular base of the coaxial transmission line using the reflow properties of solder, and imprinting the stamp produced smooth rounded terminations. Copper shielding was electroplated and a sacrificial photosensitive polycarbonate was patterned using a unique interaction with the copper. The polycarbonate was over-coated with a epoxycyclohexyl polyhedral oligomeric silsesquioxane (POSS) layer and then thermally decomposed to form an air cavity. A center conductor was patterned using photolithography and electro-deposition. The half-coaxial line was aligned with a sample with the top portion of the copper shielding and bonded in the imprinter to complete the structure. Imprint lithography also demonstrated the capability to planarize surfaces which simplified the buildup process, and complex structures were fabricated with a comparable number of registration steps to traditional transmission lines. The mechanical integrity of the air-clad transmission lines was also evaluated using nano-indentation.

1. Introduction

Because of the large data requirements of high performance computing systems, bandwidth needs for future systems are expected to expand in the next decade. As the frequency of input–output (I/O) connections increases, there will be a need for high speed connections between system components and the network that do not hinder circuit performance. Advanced connections are especially needed for systems with large distances between components where signal strength can degrade considerably. Both optical and electrical connections are used for high-speed communication between chips or networks. Optical links are preferred for long transmission lengths because optical fibers have low loss. Additionally, a fiber can transmit multiple data sets and therefore attain higher data rates than electrical connections. However, at short transmission lengths, integration of optical connections can be challenging due to the rigorous alignment tolerances and losses at sharp routing angles [1].

Implementing electrical connections lessens integration challenges, but signal loss must be reduced to be viable. Traditionally, transmission lines on printed circuit boards are micro-strip lines shown in Fig. 1(a) that are fabricated with copper and an insulating dielectric. The signal does not merely propagate on the conductor but between the conductor and the reference plane in the form of an electric and a magnetic field. Since the conductor is not infinitely conductive and the dielectric is not infinitely resistive, losses arise in the signal. The loss in the dielectric scales linearly with frequency, the loss in the conductor scales with the square root of frequency, and at operating frequencies above 10 GHz the loss in the dielectric becomes the dominant loss contribution [2].

According to the International Technology Roadmap for Semiconductors off-chip operating frequencies will exceed 9.5 GHz by 2010 and 88 GHz by 2020 [3]. At these high operating frequencies, the power loss dissipated limits the maximum distance the signal can be routed at the necessary signal to noise ratio. Furthermore, as channel density increases to maximize the data rate, cross-talk and radiation losses become considerable. Due to power loss in the transmission line and cross talk, low loss structures are needed for high frequencies, long transmission lengths, or high density applications. To minimize crosstalk noise, radiation losses, and power loss, transmission lines must have electrical shielding and insulators that provide low capacitance and inductance.

Coaxial transmission lines shown in Fig. 1(b) are commonly used in radio frequency (RF) systems because they contain the propagating electromagnetic signal and consequently do not radiate noise or pick up other signals in their vicinity. Fabricating a coaxial line using traditional microelectronics fabrication techniques is challenging due to the three dimensional structure of the coax. Researchers have demonstrated coaxial lines on a monolithic scale and have used complex photolithographic techniques to fabricate half-coaxial structures [4,5].

* Corresponding author.
E-mail address: kohl@gatech.edu (P.A. Kohl).

0167-9317/$ - see front matter © 2010 Elsevier B.V. All rights reserved.
doi:10.1016/j.mee.2010.10.040

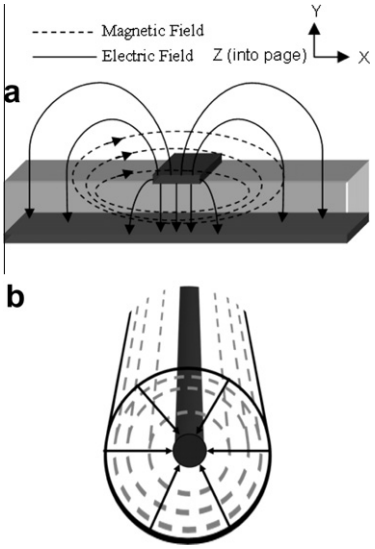

Fig. 1. Schematic of electrical and magnetic fields for a transmission line. (a) Microstrip transmission line and (b) coaxial transmission line.

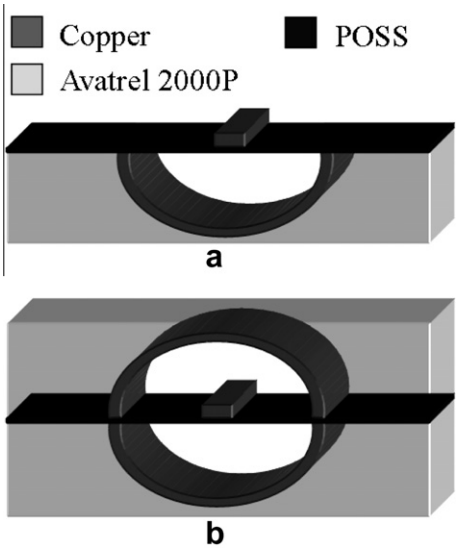

Fig. 2. Schematic of constructed (a) half-coaxial and (b) air-clad coaxial transmission line.

In this work, sacrificial polymers and the unique three dimensional patterning capabilities of imprint lithography have been used to fabricate the transmission lines shown in the schematics illustrated in Fig. 2(a) and (b). The inclusion of an air gap can mitigate dielectric loss allowing the signal to propagate over longer lengths or at higher frequencies [6]. Additionally, the low dielectric constant of air lowers the loss contributions from the conductor and increases the signal propagation velocity reducing delay. The use of sacrificial polymers and imprint lithography is compatible with board processing and has similar masking and registration steps to traditional transmission line fabrication. The imprint process can also leave uniform dielectric material thicknesses while improving line definition allowing lower tolerances for impedance control. The development of this process for advanced packaging applications could advance integrated circuit performance capabilities with high throughput and yield while maintaining low cost.

2. Experimental and material selection

To create the semicircular stamp for imprinting, a full seed layer of Ti/Au/Ti (300 Å/3000 Å/300 Å) was sputtered using the Unifilm sputtering system onto glass wafers. A 1.5 μm layer of oxide was deposited using the Unaxis PECVD and rectangular lines were photopatterned using NR-9 (Futurexx). The NR-9 was spin-coated to a thickness of 30 μm and soft baked at 110 °C for 30 min. The resist was photopatterned at 400 mJ/cm^2 using the Karl Suss MA-6 Mask Aligner which uses a 350 W mercury lamp that exposes across the spectrum 230–400 nm. The sample was then post-exposure baked for 20 min at 75 °C, and developed in RD-6 (Futurexx) to define rectangular trenches. The oxide and titanium in the exposed region were wet etched back using buffered oxide etch solution, and tin/lead solder lines were electroplated. The photoresist was stripped in acetone, and flux (Rector Seal) was used to reflow the lines at 230 °C to achieve the semi-circular geometry. The stamp was coated with Teflon AF (DuPont) and soft baked at 115 °C for 10 min.

Imprint materials were selected for their ability to replicate and retain mold patterns, and Avatrel 2000P serves as the primary imprint material for this structure. Avatrel 2000P is a polynorbornene based negative-tone, photosensitive, dielectric material developed by Promerus LLC. The general chemical structure is illustrated in Fig. 3(a). The polymer is a random copolymer in which each of the seven-member norbornene rings on the backbone is functionalized with either alkyl or epoxide side groups. The properties of the polymer film can be controlled by varying the ratio of alkyl to epoxide side groups that are substituted directly to the polymer backbone. The polymer has a dielectric constant of 2.5, and a glass transition temperature above 250 °C [7].

To fabricate the transmission line, a polynorbornene polymer Avatrel 2000P was spin coated to a thickness of 30 μm and soft baked at 100 °C for 15 min. The semi-circular stamp was imprinted into the soft baked Avatrel 2000P film at 110 °C and 45 bar for 60 s

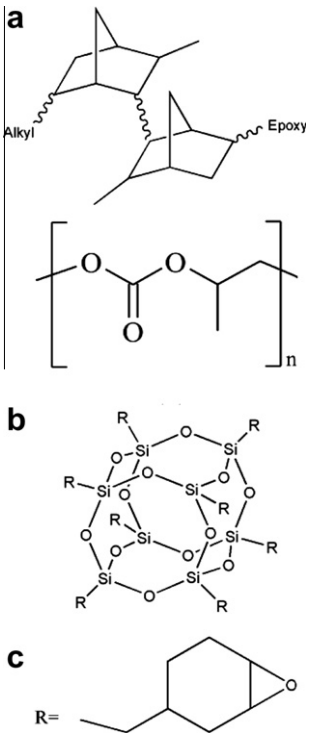

Fig. 3. Chemical structures of polymers used in fabrication. (a) Avatrel 2000P, (b) polypropylene carbonate and (c) epoxycyclohexyl POSS.

using the Obducat Imprint Lithography System. The imprinted polymer sample was blanket exposed to 365 nm ultra-violet (UV) light at 300 mJ/cm^2 using the Optical Associates Inc. Mask Aligner and post-exposure baked in an oven at 100 °C for 20 min. A seed layer of Ti/Cu (300 Å/3000 Å) was sputtered using the CVC DC Sputterer and electroplated to 1.5 μm. Mechanical polishing with 0.05 μm alumina slurry was used to remove copper from the field leaving copper solely in the trench. The sample was quickly rinsed in a 3% sulfuric acid and 3% hydrogen peroxide solution to remove copper oxide and debris.

Polypropylene carbonate (PPC) serves as a place holder for the air cavities because it can be decomposed thermally. PPC, shown in Fig. 3(b), is an aliphatic polycarbonate produced through copolymerization of carbon dioxide and propylene oxide. The thermoplastic material has an elastic modulus of 2 GPa, a dielectric constant of 3, and a glass transition temperature of 40 °C [8]. PPC can be used as a sacrificial material and complete thermal decomposition of PPC occurs at 250 °C [8]. The addition of photo-acid generator has been shown to decrease the onset of thermal decomposition [9] and so a 3% weight loading of photo-acid generator was added to the PPC formulation. The primary volatile products of decomposition are acetone and carbon dioxide and can permeate through many dielectrics at the decomposition temperature [10].

A thick layer of PPC was spin-coated onto the imprinted sample and soft baked at 115 °C for 15 min. Teflon AF (DuPont) was coated onto a blank glass slide and baked at 115 °C for 10 min. The flat glass slide was used to press the sacrificial PPC material into the trench and planarize the field at 60 °C and 45 bar for 180 s in the Obducat Imprint Lithography System. The sample was blanket exposed to 365 nm UV light at 1000 mJ/cm^2 using the Optical Associates, Inc. Mask Aligner, and the PPC was allowed to decompose from the field region on a hotplate at 180 °C for 15 min.

A photodefinable epoxycyclohexyl polyhedral oligomeric silsesquioxane (POSS) (Hybrid Plastics Inc.), shown in Fig. 3(c), was used for suspending the transmission line in the air cavity due to its mechanical strength coupled with its optimal strain and stress properties [11]. The epoxy functionalized dielectric material along with an iodonium photo-acid generator and a 365 nm sensitizer yields photo-definable, highly cross-linked films [11]. POSS was spin-coated onto the sample to a 3 μm thickness and soft baked for 6 min at 85 °C. The sample was exposed to UV light at 400 mJ/cm^2 using the Optical Associates Inc. Mask Aligner. A seed layer of Ti/Cu/Ti (300 Å/3000 Å/300 Å) was sputtered using the CVC DC Sputterer. The sample was then photo-patterned with NR-9 to a 15 μm thickness and soft baked at 110 °C for 30 min. The resist was aligned and photo-patterned at 400 mJ/cm^2 using the Karl Suss MA-6 Mask Aligner; the sample was post-exposure baked for 20 min at 75 °C, and developed in RD-6 (Futurexx) to define rectangular trenches. The titanium in the exposed region was wet etched back using buffered oxide etch solution, and copper lines were electroplated. The photo-resist was stripped in acetone and the titanium seed layer was etched using buffered oxide etch solution, and the copper seed layer was etched back in a 3% sulfuric acid and 3% hydrogen peroxide solution.

The PPC in the trench was slowly decomposed in a nitrogen furnace purged to 1 ppm oxygen. The chosen stepwise recipe maintains the decomposition at 0.25 wt.% per min. The sample was ramped to 140 °C at 1 °C/min and held at temperature for 4 h; ramped to 160 °C at 1 °C/min and held at temperature for 2 h; ramped to 180 °C at 1 °C/min and held for 5 h. The furnace was allowed to cool slowly by natural convection to room temperature.

Quasi-static nano-indentation was conducted using a Hysitron Triboindenter. Indentations on Avatrel 2000P polymer samples were performed with a Berkovich tip and loaded to 1000 μN over five points per sample. A maximum drift rate of 0.1 nm/s of was set for the experiment and was automatically determined over a 40 s period. The tip was loaded to maximum load in 10 s, held for 10 s, and unloaded in 2 s. The load–depth curves were analyzed using the Oliver–Pharr model to obtain the reduced modulus (E_r) and the hardness (H) [12]. Indentations on air cavities were performed using a 60° cono spherical tip and samples were ramped to a force of 8750 μN in 10 s and then unloaded in 10 s.

To complete the top portion of the copper shielding, Avatrel 2000P was spin coated to a thickness of 30 μm and soft baked at 100 °C for 15 min. The semi-circular stamp was imprinted into the soft baked Avatrel 2000P film at 110 °C and 45 bar for 60 s using the Obducat Imprint Lithography System. A seed layer of Ti/Cu (300 Å/5000 Å) was sputtered using the Unifilm Sputterer and electroplated to a total thickness of 1.5 μm. The sample was then photopatterned with AZ-4620 (AZ Electronic Chemicals) to a 10 μm thickness and soft baked at 90 °C for 10 min in an oven. The resist was aligned and photopatterned at 900 mJ/cm^2 using the Karl Suss MA-6 Mask Aligner and developed in AZ-400 K (AZ Electronic Chemicals). The copper seed layer was etched back in a 3% sulfuric acid and 3% hydrogen peroxide solution, and the resist was stripped in acetone. The top portion of the copper shielding was bonded with the half-coaxial line in the imprinter at 160 °C, 15 bar, for 180 s. The sample was then cured in a furnace with a ramp to 160 °C at 5 °C/min and held at temperature for 1 h. The furnace was allowed to cool slowly by natural convection to room temperature.

For samples with the photo-resist release layer, NR-9 was spin-coated to a thickness of 30 μm and soft baked at 110 °C for 30 min. Processing then followed the procedure dictated for the top portion of the copper shielding. To release the top wafer from the bonded transmission line, the sample was placed in acetone in an ultra-sonic bath for 3 min. For samples with the photo-sensitive tape release layer, the UC-120m-120 (Furukawa Electric) UV sensitive tape was used. The tape was bonded onto a glass substrate in the imprinter at 125 °C, 15 bar, for 180 s and processing then followed the procedure dictated for the top portion of the copper shielding. To release the top wafer, the sample was exposed to UV light at 1000 mJ/cm^2 using the Optical Associates Inc. Mask Aligner.

A Zeiss Ultra 60 and Hitachi 3500H were used to obtain scanning electron microscope (SEM) images of the processed films. Thermal stability characterization was conducted via thermal gravimetric analysis (TGA) using a TA instruments Q50. The materials were heated to 300 °C using a 1 °C/min ramp rate and a nitrogen atmosphere.

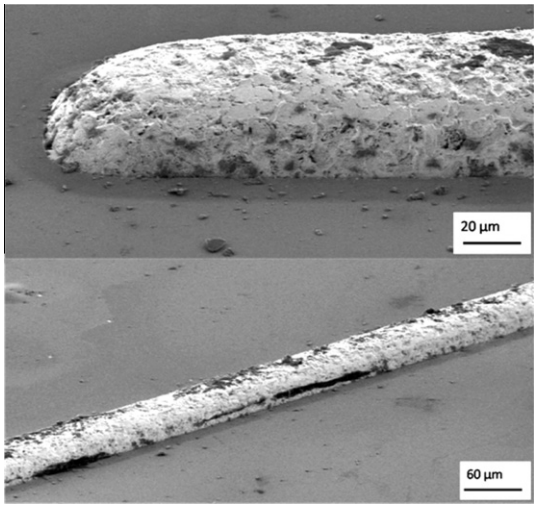

Fig. 4. SEM images of 50 μm wide solder imprint stamp.

3. Results and discussion

To begin building the ultra-low loss transmission line, an imprint stamp was fabricated to create the base of the coaxial structure. Photolithography could have been used to pattern the structure. However, straight lines with sharp corners are electrically unfavorable at terminations and discontinuities where reflections could occur, and these power losses become significant at high frequencies. To fabricate a semi-circular trench in the film, a stamp with a semi-circular line was made using solder. At temperatures above the alloy's melting point and upon removal of surfaces oxides, solder will form a spherical shape in order to minimize its surface forces. By utilizing this behavior, tin–lead solder rectangular lines were electroplated and then reflowed to achieve a rounded geometry. As shown in Fig. 4, there is a small amount of surface roughness of the line, but this could be eliminated with further optimization of reflow conditions or bath chemistry. The stamps were then coated with Teflon AF to facilitate easy separation after imprinting.

The negative-tone polynorbornene, Avatrel 2000P, serves as the base material for imprinting the trench because of its thermosetting properties and low dielectric constant. Avatrel 2000P polymer properties change during soft-bake, UV exposure, post-exposure bake, and cure. To ensure proper pattern transfer into the dielectric, the optimal processing step for imprinting into the material had to be determined. Nano-indentation experiments were conducted after each of the four processing steps to determine the optimal Avatrel 2000P process step for imprinting. For a fixed force of 1000 μN, the Berkovich tip displaced 998 nm after soft bake, but only about 800 nm after exposure and post-exposure bake, and 672 nm after cure. The mechanical properties were determined from force–displacement curves and are summarized in Table 1. The indentation depth data suggest that imprinting after polymer soft-bake displaces the most material for a given force. Therefore, imprinting was conducted after polymer soft bake, because it requires the least force to displace material.

Ideally, imprint processes would occur at atmospheric pressure and ambient temperature. However, deforming polymers at these conditions is very time consuming. To enable mold filling, thermal imprint lithography is typically conducted at 50–70 °C higher than the glass transition temperature of the imprint material [13]. Avatrel 2000P is a photosensitive dielectric that is processed at 100 °C and cured at 160 °C, and the glass transition temperature of the cured material is above 250 °C. Operating at temperatures much higher than the photo-processing conditions can initiate thermal crosslinking of the material, and as the indentation data suggested, the cross-linked polymer chains are more difficult to displace than the non-cross-linked material.

A range of temperatures and pressures were evaluated for best resolution of features, while avoiding thermal cross-linking of the material during imprinting. Imprinting at 110 °C, 45 bar for 60 s into a soft-baked film of Avatrel 2000P accurately transferred the stamp pattern and had the good planarity in the non-imprinted region. The sample was then blanket exposed to UV light and post-exposure baked. As shown in Fig. 5, the roughness of the imprinted feature replicates stamp roughness, but smoother lines can be achieved by refining stamp fabrication.

Table 1
Nano-indentation results of Avatrel 2000P after each processing step for a fixed force of 1000 μN with a Berkovich tip.

Step	Depth (nm)	E_r (GPa)	H (GPa)
Soft-bake	998	0.56	0.018
Exposure	822	0.68	0.028
PEB	803	0.74	0.029
Cure	672	0.96	0.043

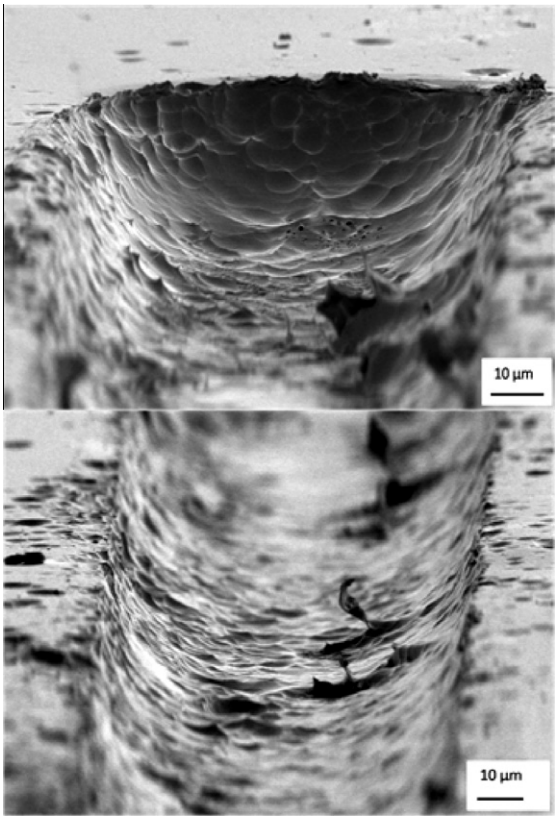

Fig. 5. SEM images of the semi-circular trench imprinted in Avatrel 2000P at 110 °C, 45 bar for 60 s.

To provide electrical shielding for the transmission line, copper was metalized on the imprint sample, and mechanical polishing was used to remove copper from the field regions. The recess of the structure protects the copper in the trench during polishing, reducing the need for patterning and registration steps. This thin layer of copper will minimize electrical interference by confining the signal from the core conductor within the structure and by also impeding outside signals from entering the line.

Furthermore, the inclusion of air dielectric layers in the transmission line lowers the effective dielectric constant, minimizing loss in both the dielectric and the conductor. To encapsulate air cavities, sacrificial polymers are used as space holders, but care must be taken to ensure that decomposition of the sacrificial material is compatible with other materials and processes. Reed et al. demonstrated the use of polycarbonates as a sacrificial material with a polymeric overcoat such a polynorbornene polymer Avatrel [14]. However, the decomposition temperature for the polycarbonates was 285 °C making them challenging to implement with existing printed circuit board materials. Jayachandran et al. were able to reduce the decomposition temperature of polycarbonates through the addition of photo-acid generator, and air cavities encapsulated with Avatrel were fabricated at temperatures below 180 °C [9]. To make the air dielectric layers suitable for printed circuit board materials, the sacrificial polymer PPC with a small amount of photo acid generator was used as a space holder for air cavities in the transmission line.

Incorporating the air dielectric layers requires the fabrication of a multi-layered structure; however, maintaining planarity across multiple film layers is challenging with traditional processing techniques. Planarity is critical for the ultra-low loss transmission line

because non-planarity of the sacrificial PPC layer could cause the overcoat layer to be non-planar. Since the overcoat layer acts as a support for the transmission line, non-planarity compromises the mechanical integrity of the transmission line. Several methods were tested to fill PPC into the imprint trench, and the planarity of the PPC layer was subsequently evaluated. Initially, a thick layer of PPC was spin-coated and soft-baked onto the imprint sample, but the film surface was uneven making it difficult to pattern and proceed with processing. Stencil filling the cavity was also attempted by taking a blade and pushing the spin-coated PPC into the cavity. However, under examination in SEM the imprinted trench filled with PPC was recessed when compared to the field region. To increase the planarity of PPC in the trench, a thick layer of PPC was spin-coated, and a flat glass slide was used to press the PPC into the trench using the imprinter at 60 °C, 45 bar for 180 s. The imprinting temperature was above the glass transition temperature of PPC causing the material to reflow into the cavity and become planar with the field.

Once a planar layer of PPC was fabricated, the PPC was patterned using a unique interaction with the patterned copper in the trench to minimize masking and registration steps. It has been shown that the thermal decomposition of some PPC mixtures in contact with a copper surface is stabilized at elevated temperature [15]. That is, the rate of thermal decomposition of the PPC is slowed resulting in the opportunity for self-patterning on copper surfaces. PPC films that were spin-coated and soft baked on a blank silicon wafer decomposed at approximately a 160 °C. PPC films that were spin-coated and soft baked on a layer of oxide-free copper had considerably higher decomposition temperatures around 225 °C. The copper only interacts with a limited PPC surface area, and some of the PPC decomposes at the lower temperature as shown in Fig. 6. Spencer suggests that the copper interferes with the chain un-zipping reaction of PPC as it decomposes causing the bulk film to decompose at higher temperatures [15].

Since the decomposition of PPC on copper and PPC on Avatrel 2000P are different, the PPC was thermally patterned on a hotplate at 180 °C, and the PPC on Avatrel 2000P decomposed, while it was preserved in the copper trench. Since the copper only affects the PPC near its surface and does not completely prevent decomposition, excess PPC in the trench decomposes. Furthermore, because the decomposition temperature is well above the glass transition temperature of the material, the PPC reflows until it is planar with the field. Fig. 6 illustrates an imprinted sample with PPC preserved in the trench region and a thin layer of gold for imaging.

After thermal patterning of the sacrificial material PPC, a thin layer of POSS was spin-coated and photo-processed to act as a support for the copper transmission line. As noted by Fritz et al. the modulus and hardness of POSS films after post-exposure bake is 4.9 GPa and 0.56 GPa, and after curing the modulus and hardness

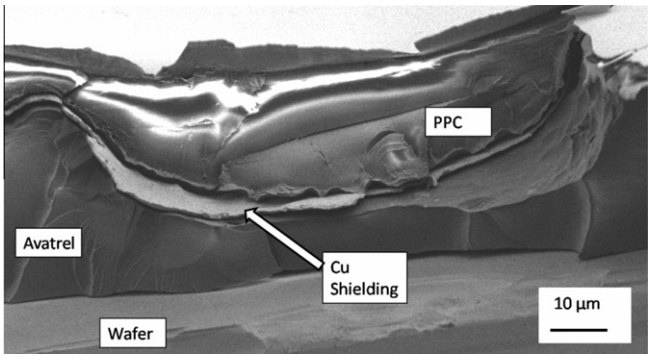

Fig. 6. SEM image of a cross-sectioned, copper-clad, semi-circular trench with patterned PPC in trench and a layer of gold for imaging.

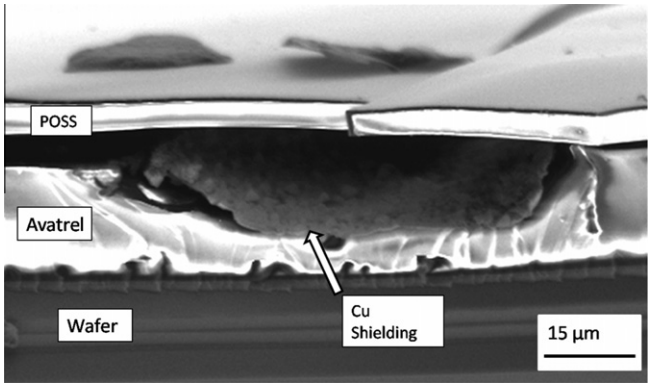

Fig. 7. SEM image of a cross-sectioned decomposed half coaxial air cavity. The crack in the POSS cavity is due to excessive cavity pressure during decomposition.

increase to 5.3 GPa and 0.64 GPa [11]. Due to the high mechanical strength of POSS, thin layers of film on the order of a few microns can support the transmission line. As a result, the ratio of air to polymer in the cavity can be maximized after PPC decomposition, reducing the effective dielectric constant and power loss.

Decomposing PPC through the POSS overcoat initially resulted in damage to the POSS overcoat as shown in Fig. 7. Decomposing the sacrificial material quickly can cause a pressure disparity between the air cavity and atmosphere leading to overcoat adhesion loss, ruptures, or cracking. To prevent cavity damage, the decomposition process was modified from a constant heat rate to a constant weight percent decomposition rate. By using a constant decomposition rate process, the diffusion of material through the overcoat is relatively constant, and therefore a pressure imbalance is less likely to occur. To redesign the decomposition recipe, thermogravimetric analysis of the polymer was conducted to determine kinetic parameters as recommended by Wu et al. [16]. The reaction kinetics for the thermal decomposition of PPC was expressed as the nth order Arrhenius relationship shown in Eq. (1) and the decomposition rate was assumed to be equal to a constant r.

$$r = Ae^{\frac{-E_a}{RT}}(1-rt)^n \tag{1}$$

The decomposition reaction was determined to be first order (n) with the pre-exponential factor (A) and activation energy (E_a) to be $9 \times 10^{12}\,\mathrm{min}^{-1}$ and 120 kJ/mol, respectively. Eq. (1) was rearranged for temperature (T) vs. decomposition time (t) as shown in Eq. (2).

$$T = \frac{E_a}{R}\left[ln\frac{A(1-rt)^n}{r}\right]^{-1} \tag{2}$$

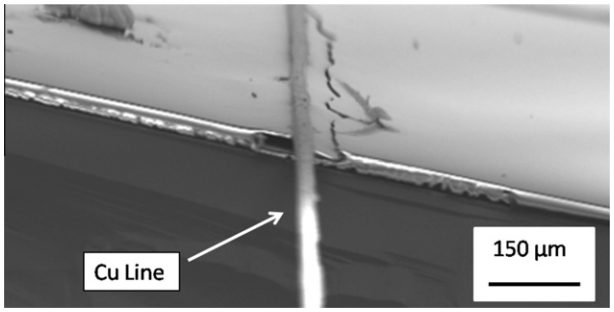

Fig. 8. SEM image of a cross-sectioned half coaxial transmission line. The copper transmission line extends beyond the sample. The crack in the POSS overcoat is due to cross-sectioning of the sample.

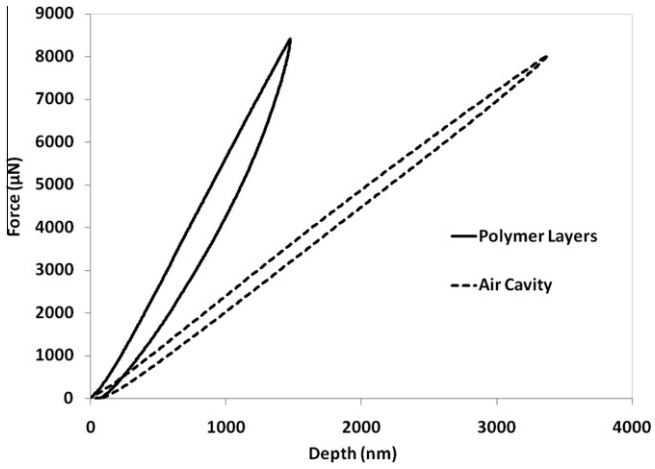

Fig. 9. Force versus displacement curves using a cono-spherical tip with a maximum force of 8750 μN for a fully constructed polymer field (solid line) and a POSS over-coated air cavity (dashed line).

The decomposition rate was set to 0.25 wt.% per min, and a step and hold recipe temperature was designed using Eq. (2). A final temperature hold was added at the end of the recipe to ensure a full decomposition, and the modified decomposition recipe provided a clean cavity without visible overcoat damage.

After successful fabrication of the air cavity, the transmission line was patterned using traditional lithography and electroplating. X-ray tomography confirmed that the transmission line was successfully patterned over the air cavity. However, obtaining cross sectional SEM images required cleaving the sample resulting in damage to the structure. As shown in Fig. 8, the copper transmission line extends from the air cavity, and the field is planar with damage only in the cleaved area.

To evaluate the mechanical integrity of the half-coaxial structures, push tests were conducted using a nano-indenter with a cono spherical tip to prevent piercing of the overcoat as recommended by Bakir et al. [17]. A triangular load function with a 10 s ramp to 8750 μN and a 10 s ramp to zero force was used to test the structures. To have a reference for comparison, push tests were initially conducted on the imprint sample over the Avatrel 2000P and POSS polymer layers and then on the air cavities with

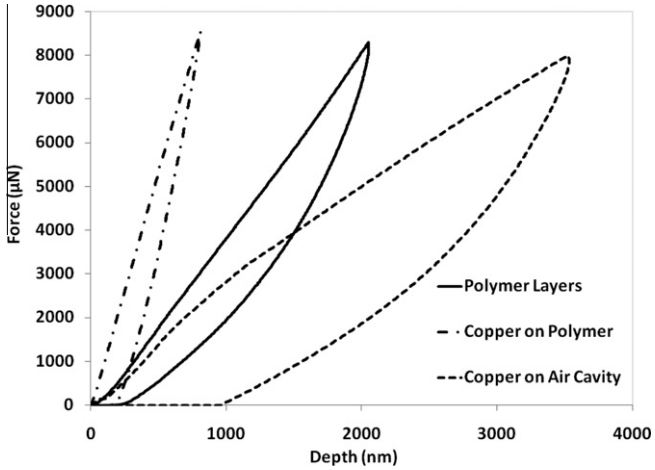

Fig. 10. Force versus displacement curves using a cono-spherical tip with a maximum force of 8750 μN for a fully constructed polymer field (solid line), copper line in the polymer field (dot-dashed line), and the copper line on the air cavity (dashed line).

no transmission line. As shown in Fig. 9, the indentation of the air cavity displaced 3500 nm and recovered quickly, which is 2000 nm greater than the indentation conducted on the polymer layers. Repeated indentations were attempted on the samples, but the displacement exceeded the maximum displacement on the equipment of 4500 nm. Under examination in a microscope, no visible damage could be seen on samples from the repeated push tests. Indentations were subsequently conducted on samples with a copper transmission line on the air cavity and on a copper line on the polymer layers. To account for variations in samples, an indentation on the Avatrel 2000P and POSS polymer layers was also repeated. As shown in Fig. 10, the copper line on the polymer layers displaced less than 500 nm, whereas the copper line over the air cavity displaced 3500 nm. The copper line does not appear to compromise the mechanical integrity of the air cavity, but due to the slow recovery of copper the indentation samples recovered slowly.

To fabricate a fully encapsulated ultra-low loss transmission line, the half-coaxial transmission line was sealed with a copper-lined trench in the imprinter. Researchers have demonstrated that imprint lithography can be used to thermally bond layers of material to create nano-fluidic channels with SU-8 [18,19]. The structure could be built up, but bonding the two halves of the transmission line together reduces processing and registration steps. Furthermore, the air-clad transmission line in this process is embedded in a planar layer of polymer simplifying the subsequent build of structures and layers in the printed circuit board.

The top half of the structure was fabricated by using a soft-baked film of Avatrel 2000P imprinted with the coaxial trench. As noted earlier, Avatrel 2000P properties change during processing, and the adhesive strength of the material decreases significantly after exposure. Therefore, the sample was sputtered and electroplated with a thin layer of copper after soft-bake. However, the copper shielding could not be patterned via mechanical polishing because the uncured polymer layer could not withstand the abrasive forces. Therefore, the copper trench was patterned via photolithography and wet etching. The Avatrel 2000P layer was not photo-patterned during this step, since the copper layer prevented the transmission of light. The copper-lined trench was then flipped, aligned, and bonded with the half-coaxial line in the imprinter at 160 °C, 15 bar for 180 s. At this elevated temperature, thermal cross-linking of the material is initiated, and curing was then conducted on the sample in a furnace at 160 °C for one hour. The imprinting pressure was set at 15 bar, which is the minimum on the equipment, to ensure that the POSS layer would not be damaged during imprinting, even if misalignment of the layers occurred. Samples were attempted to be separated after bonding and after cure, but the substrates would crack before the polymer interfaces would delaminate, suggesting good adhesion between the layers. Cross-sectioning via dicing and polishing were attempted of the complete structure, but the POSS layer could not withstand these techniques making imaging of the complete structure difficult.

Several release layers were also tested for removing the top substrate off the ultra-low loss transmission line. Photosensitive tapes and photo-resist both demonstrate potential as a sacrificial release layer for this application. To use the photo-resist as a sacrificial release layer, a layer of NR-9 was spin-coated onto the substrate before coating of the Avatrel 2000P. This material was chosen because it has similar processing conditions to the Avatrel 2000P and was not miscible in the developer used to photo-pattern the copper trench. Samples imprinted with the NR-9 layer showed no changes in the resolution of the imprinted features. After bonding with the half-coaxial line, the NR-9 was dissolved in acetone in an ultra-sonic bath for 3 min. No damage to the encapsulated cavity was observed, and the Avatrel 2000P remained adherent to the

POSS Layer. On an industrial scale, using a soluble release layer could be challenging as transport would be limited as sample size increased. Photo-sensitive tapes were also tested as a sacrificial release layer. Photo-sensitive tapes have strong adhesive strength that are reduced significantly after UV irradiation and are used in industrial applications for wafer dicing and grinding. To use as a release layer, the photo-sensitive tape was bonded onto a transparent substrate in the imprinter, and the Avatrel 2000P was subsequently spin-coated and processed. On the lab scale, obtaining a completely planar layer was challenging. During bonding in the imprinter, bubbles and wrinkles would be entrapped in the layer making planarity a challenge during subsequent processing. However on an industrial level, these issues could be resolved with the proper equipment. An additional challenge of implementing the photo-sensitive tape is managing the coefficient of thermal expansion mismatch between the layers. Rapid heating and cooling caused buckling of the photo-sensitive tape from the carrier substrate in some samples.

4. Conclusion

Imprint lithography and sacrificial polymers have been used to fabricate a novel structure with smooth transitions, metallic shielding, and encapsulated air dielectric layers. Using imprint lithography, the semi-circular geometry was transferred into Avatrel 2000P with only elevated temperature and pressure. Curved structures are difficult to make using traditional photolithography which demonstrates the potential of imprint lithography to build complex geometries. The rounded terminations can be integrated with vertical connections with smooth transitions that will reduce reflections and therefore increase power transmission. Additionally, the imprint process planarized surfaces simplifying the buildup process and is compatible with traditional board processing. Furthermore, the natural relief of the structure allowed the copper shielding in the trench to be patterned using simple mechanical polishing eliminating a masking and registration step. Sacrificial polymers were encapsulated in copper and Avatrel 2000P. Air insulation layers can lower the effective dielectric constant and therefore, reduce power loss and increase signal propagation velocities [6].

Conductor, dielectric, and radiation losses along with reflections and discontinuities must be reduced to enable high frequency chip to chip communication. This structure is the first report to incorporate features to mitigate all of these losses. The fully encapsulated air-clad transmission line can be embedded within the printed circuit board extending the benefits of air dielectrics. These processes can enable the fabrication of ultra-low loss transmission lines to increase the lengths at which the signal can be routed at the proper signal to noise ratio or increase the data rate per channel.

Acknowledgments

The authors gratefully acknowledge the support of the Interconnect Focus Center, one of six Semiconductor Research Corporation Focus Centers. The authors also acknowledge the support of Promerus LLC for providing materials for this research and many useful discussions. The authors acknowledge Tyler Osborn for his insight and guidance with the electroplating of imprint stamps; Laura Gaskins a summer undergraduate researcher from NNIN who helped fabricate several structures for this project; and Lisa Thornsberry who helped run the PPC TGA samples.

References

[1] C. Hoyeol, K. Kyung-Hoae, P. Kapur, K.C. Saraswat, IEEE Electron Device Letters 29 (2008) 122.
[2] A. Djordjevi, R. Biljie, V. Likar-Smiljanic, T. Sarkar, IEEE Transactions on Electromagnetic Compatibility 43 (2001) 662.
[3] ITRS. The International Technology Roadmap for Semiconductors http://www.itrs.net.
[4] S. Jun-De Jin, M. Yang, S. Liu, IEEE Transactions on Microwave Theory and Techniques 54 (2006) 4333.
[5] S. Natarajan, T. Weller, A. Hoff, IEEE Microwave Symposium Digest (2006) 424–427.
[6] D.M. Pozar, Microwave Engineering, third ed., John Wiley & Sons, Hoboken, NJ, USA, 2005.
[7] Promerus. Materials http://www.promerus.com/packaging_materials.asp.
[8] Empower-materials. Poly(alkylene carbonates) typical properties http://www.empowermaterials.com/download/Technical%20Information/typical_properties.pdf.
[9] J. Jayachandran, H. Reed, H. Zhen, L. Rhodes, C. Henderson, S. Allen, P. Kohl, Journal of Microelectromechanical Systems 12 (2003) 147.
[10] M. Cupta, Georgia Institute of Technology (2006).
[11] N. Fritz, R. Saha, S. Allen, P. Kohl, Journal of Electronic Materials 39 (2010) 149.
[12] W. Oliver, G. Pharr, Journal of Materials Research 7 (1992) 1564.
[13] H. Schift, S. Bellini, J. Gobrecht, F. Reuther, M. Kubenz, M.B. Mikkelsen, K. Vogelsang, Microelectronic Engineering 84 (2007) 932.
[14] H. Reed, C. White, V. Rao, S. Allen, C. Henderson, P. Kohl, Journal of Micromechanics and Microengineering 11 (2001) 733.
[15] T. Spencer, Y. Chen, R. Saha, P.A. Kohl, Stabilization of the thermal decomposition of poly(propylene carbonate) through copper ion incorporation and use in self-patterning. Submitted advanced materials.
[16] X. Wu, H. Reed, Y. Wang, L. Rhodes, E. Elce, R. Ravikiran, R. Shick, C. Henderson, S. Allen, P. Kohl, Journal of the Electrochemical Society 150 (2003) H205.
[17] M.S. Bakir, H.A. Reed, H.D. Thacker, C.S. Patel, P.A. Kohl, K.P. Martin, J.D. Meindl, IEEE Transactions on Electron Devices 50 (2003) 2039.
[18] X. Wang, L. Ge, J. Lu, X. Li, K. Qiu, Y. Tian, S. Fu, Z. Cui, Microelectronic Engineering 86 (2009) 1347.
[19] J. Hoff, L. Cheng, E. Meyhofer, L. Guo, A. Hunt, Nano Letters 4 (2004) 853.